*Inflammation, Vol. 45, No. 1, February 2022 (© 2022)*
https://doi.org/10.1007/s10753-021-01548-2

ORIGINAL ARTICLE

# Exosomes Derived from ADSCs Attenuate Sepsis-Induced Lung Injury by Delivery of Circ-Fryl and Regulation of the miR-490-3p/SIRT3 Pathway

**Weijun Shen[1] , Xuan Zhao[2] and Shitong Li[1,3]**

*Received 24 April 2020; accepted 16 August 2021*

*Abstract*——Sepsis-induced lung injury is a clinical syndrome characterized by injury of alveolar epithelium cells (AECs). Previous investigations illustrate that exosomes secreted from adipose-derived stem cells (ADSCs) have therapeutic effects in a variety of disease treatments, but roles and mechanisms regarding ADSC-derived exosomes in sepsis-induced lung injury are unclear. In this study, high-throughput sequencing was used to explore the molecular delivery of ADSC exosomes. A sepsis-induced lung injury mouse model and a lipopolysaccharide-induced AEC damage model were used for mechanistic analysis. The results showed that ADSC exosomes have high levels of the circular RNA (circ)-Fryl. Downregulation of circ-Fryl suppressed ADSC protective effects exosomes against sepsis-induced lung injury by decreasing apoptosis and inflammatory factor expression. Bioinformatics and luciferase reporting experiments showed that miR-490-3p and SIRT3 are downstream targets of circ-Fryl. miR-490-3p overexpression or SIRT3 silencing reversed ADSC exosome protective effects. Studying the mechanism showed that overexpression of circ-Fryl promoted autophagy activation by inducing SIRT3/AMPK signaling. Autophagy activation can suppress sepsis-induced lung injury by decreasing apoptosis and inflammatory factor expression. Taken together, our results suggest that exosomes derived from ADSCs attenuate sepsis-induced lung injury by delivery of circ-Fryl and regulation of the miR-490-3p/SIRT3 pathway.

**KEY WORDS:** exosomes; sepsis; lung injury; circ-fryl; SIRT3.

## INTRODUCTION

Sepsis is a systemic inflammatory response syndrome (SIRS) that is the result of infection. Epidemiological survey data suggest that sepsis affects 750,000 patients in USA every year; approximately 9% develop severe sepsis and 3% develop septic shock [1]. The sepsis incidence in Chinese intensive care units is 8.68% and the mortality ratio can be as high as 50% [1, 2]. Sepsis can damage multiple organs, and the lungs are often the first

[1]Nanjing Medical University, Shanghai General Hospital, Shanghai 200080, China
[2]Department of Anesthesiology, Tenth People's Hospital of Tongji University, No 301 Middle Yan Chang Road, Shanghai 200072, China
[3]Nanjing Medical University, Shanghai General Hospital, Shanghai 200080, China

target. However, sepsis-induced lung injury remains difficult to treat, as the disease pathophysiology is unknown.

Previous studies have shown that apoptosis and the inflammatory response of alveolar epithelial cells (AECs) play important roles in sepsis-induced lung injury [3, 4]. Enhancing autophagy will protect against sepsis-induced acute lung injury [5]. Previous studies have found that sinomenine attenuates sepsis-associated lung injury via autophagy and Nrf2/Keap1 [6]. Thus, activation of autophagy may help inhibit sepsis-induced lung injury.

Several preclinical studies have shown that mesenchymal stem cell-derived exosomes, which have angiogenic, immunomodulatory, anti-inflammatory, and paracrine effects, protect organ function following injury [7–9]. ADSCs are considered adipose-derived stromal cells that are multipotent and can differentiate into various cell types including chondrocytes, osteoblasts, and adipocytes. With potential application of ADSCs in tissue repair and regeneration, they include perfect ability regarding inflammatory or autoimmune diseases regulation. A previous study showed that microRNA (miRNA)-126-modified ADSC-derived exosomes enhanced functional recovery of posterior stroke in a rat model by promoting suppressing microglia activation and neurogenesis [10]. Mmu_circ_0001359-modified ADSC exosomes attenuate airway remodeling through improving FoxO1 signaling-mediated M2-like macrophage activation [11], while the ADSC exosome role in sepsis-induced lung injury remains unclear.

The present study employed ADSC-derived exosomes to investigate exosome therapeutic effects in a sepsis-induced lung mice model. The data verified that exosomes exhibited therapeutic effects via reprogramming microenvironment through delivery of circ-Fryl and regulation of the miR-490-3p/SIRT3 pathway. SIRT3 plays an important role in promoted autophagy activation and autophagy activation can attenuate sepsis-induced lung injury. So we hypothesize that exosomes derived from ADSCs attenuate sepsis-induced lung injury by promoting autophagy activation via delivery of circ-Fryl and regulation of the miR-490-3p/SIRT3 pathway.

## MATERIALS AND METHODS

### Ethics Statement

The Animal Care and Use Committee of the Shanghai Tenth People's Hospital approved the research. We conducted postoperative animal care and treatment surgical interventions according to NIH Guide of Laboratory Animals Care and Use.

### Cell Treatment

To validate alveolar epithelial cell (AEC) apoptosis and dysfunction, 3 μg/mL lipopolysaccharide (LPS) was added to AECs in six-well plates to establish the cell model. We cultured AECs at 37 °C with $CO_2$ of 5% in Dulbecco's modified Eagle's medium (DMEM; Gibco, Grand Island, NY, USA) containing fetal bovine serum (FBS; Gibco). Cells were collected for further analysis 1 day after LPS administration.

### Strand-Specific RNA-Seq Library Construction and High-Throughput RNA-Seq

We extracted total RNA from ADSC exosomes through TRIzol reagent (Invitrogen, Carlsbad, CA, USA). We subjected 3 μg of total RNA from every sample to VAHTS Total RNA-Seq (H/M/R) Library Prep Kit from Illumina (Vazyme Biotech Co., Ltd, Nanjing, China) to erase ribosomal RNA retaining other classes of RNA such as non-coding RNA and mRNA. We treated purified RNA through RNase R (Epicenter, 40 U, 37 °C for 3 h), followed by TRIzol purification. We prepared RNA-Seq libraries via KAPA Stranded RNA-Seq Library Prep Kit (Roche, Basel, Switzerland) followed by deep sequencing via Illumina HiSeq 4000 at Aksomics, Inc. (Shanghai, China).

### ADSC Isolation and Identification

We isolated ADSCs from adipose tissue as previously described [19]. We observed no spontaneous differentiation in cultural expansion. We induced osteogenic differentiation through culturing ADSCs for 3 weeks in DMEM supplied with FBS of 10%, dexamethasone of 0.1 μM, 50 μM ascorbate-2-phosphate, and 10 mM β-glycerophosphate. We induced adipogenic differentiation through cultivating ADSCs for 2 weeks in DMEM supplemented with FBS of 10%, 10 μM insulin, 200 μM indomethacin, dexamethasone of 1 μM, and 0.5 mM isobutylmethylxanthine. We detected osteogenic or adipogenic differentiation regarding ADSCs through Oil-Red O and alkaline phosphatase staining.

## Identification and Isolation of ADSC-Derived Exosomes

We isolated ADSC-derived exosomes as formerly described [16]. At 80–90% confluency, ADSCs were rinsed with phosphate-buffered saline (PBS) and cultivated in FBS-free endothelial cell growth medium-2MV supplemented with 1 × serum replacement solution (PeproTech, Rocky Hill, NJ, USA) for 2 days. We then eliminated conditioned culture medium and centrifuged cells at 300 × *g* for 10 min and at 2000 × *g* for another 10 min to erase cellular debris as well as apoptotic cells. Following centrifugation at 10,000 × *g* for half of an hour, we filtered supernatant with 0.22 μm filter (Millipore, Billerica, MA, USA) and transferred 15 mL to Amicon Ultra-15 Centrifugal Filter Unit (100 kDa; Millipore) and centrifuged them at 4000 × *g* with ~ 1 mL concentration. Ultrafiltration unit was washed twice with PBS and we filtered supernatant again at 100,000 × *g*. We resuspended exosome pellets in 500 μL PBS; we performed subsequent procedures at 4 °C. We determined exosome protein concentration through the Pierce BCA Protein Assay Kit (Thermo Fisher Scientific, Waltham, MA, USA). We stored exosomes at − 80 °C and identified them via western blotting and transmission electron microscopy.

## Establishment of the Sepsis-Induced Lung Injury Mouse Model

Sepsis-induced lung injury mouse model, which includes cecal ligation and puncture, was generated as previously performed [12]. Following anesthesia by intraperitoneal injection of 1% pentobarbital sodium (40 mg/kg), we shaved abdominal hair with a razor, secured mice on an operating table, and disinfected abdomen with iodine and covered it with a sterile sheet. The mice were breathing spontaneously and the abdomen was opened along the midline of the mid-lower abdomen to expose the cecum. The fecal contents of the cecum were squeezed to the distal end. The inferior margin of the cecum and the cecal artery were punctured with a 6/0 silk thread at the inferior margin of the cecum and the cecum was ligated. The ileum and cecal mesenteric vessels were not ligated. The dorsal distal and proximal ends of the cecum were punctured once using an 18 F needle and the fecal contents were squeezed out. The cecum was then placed back into the abdominal cavity. The abdominal wall incision was sutured in layers. Then, sterile normal saline (5 mL/100 g) at 37 °C was subcutaneously injected to resuscitate the mice. The mice without analgesia were placed on a warming blanket after surgery. For exosome treatment, mice underwent tail intravenous injections of 200 μg exosomes from different groups of ADSCs in 100 μL PBS; we injected control mice with equivalent volume of PBS. We euthanized mice after 1 week, and harvested lung specimens for histopathological evaluation.

## TUNEL Staining

We detected apoptosis in lung tissues using a TUNEL apoptosis kit. Tissues were observed and photographed, and apoptotic cell numbers were calculated. Apoptotic cells showed yellow-green fluorescence, while normal cells showed no fluorescence.

## Bioinformatics Analyses

We predicted circular RNA (circRNA)/miRNA target genes with the http://starbase.sysu.edu.cn/ tool. We predicted interactive correlation between SIRT3 and miR-490-3p using TargetScan.

## RNA Interference or Overexpression

We obtained miR-490-3p inhibitors or mimics, circ-Fryl downregulation/overexpression vectors, and SIRT3 downregulation/overexpression vectors from RiboBio (Guangzhou, China). Transfection was performed with Lipofectamine 2000 (Thermo Fisher Scientific) as formerly described [13]. miR-490-3p and SIRT3 were determined to be downstream targets of circ-Fryl.

## Quantitative Real-Time Polymerase Chain Reaction (qPCR)

Total RNA was extracted from skin tissue or cells from the wound using the TRIzol reagent kit (Invitrogen). cDNA was synthesized and amplified using the TaqMan miRNA Reverse Transcription Kit. qPCR was conducted with the TaqMan™ MicroRNA Assay Kit (#4,440,885, Applied Biosystems, Foster City, CA, USA). We used $2^{-\Delta\Delta CT}$ method to detect expression relative fold changes. We employed *U6* and *GAPDH* as internal controls. The primers used were as follows: *circ-Fryl* forward, 5′-GTCACCACCAAGAACTTAGCCG-3′, *circ-Fryl* reverse, 5′-GCTGGGAAAAGCAGCAAGGTCAG-3′, *miR-490-3p* forward, 5′-CAGCAUGGAGUCCUCCAG

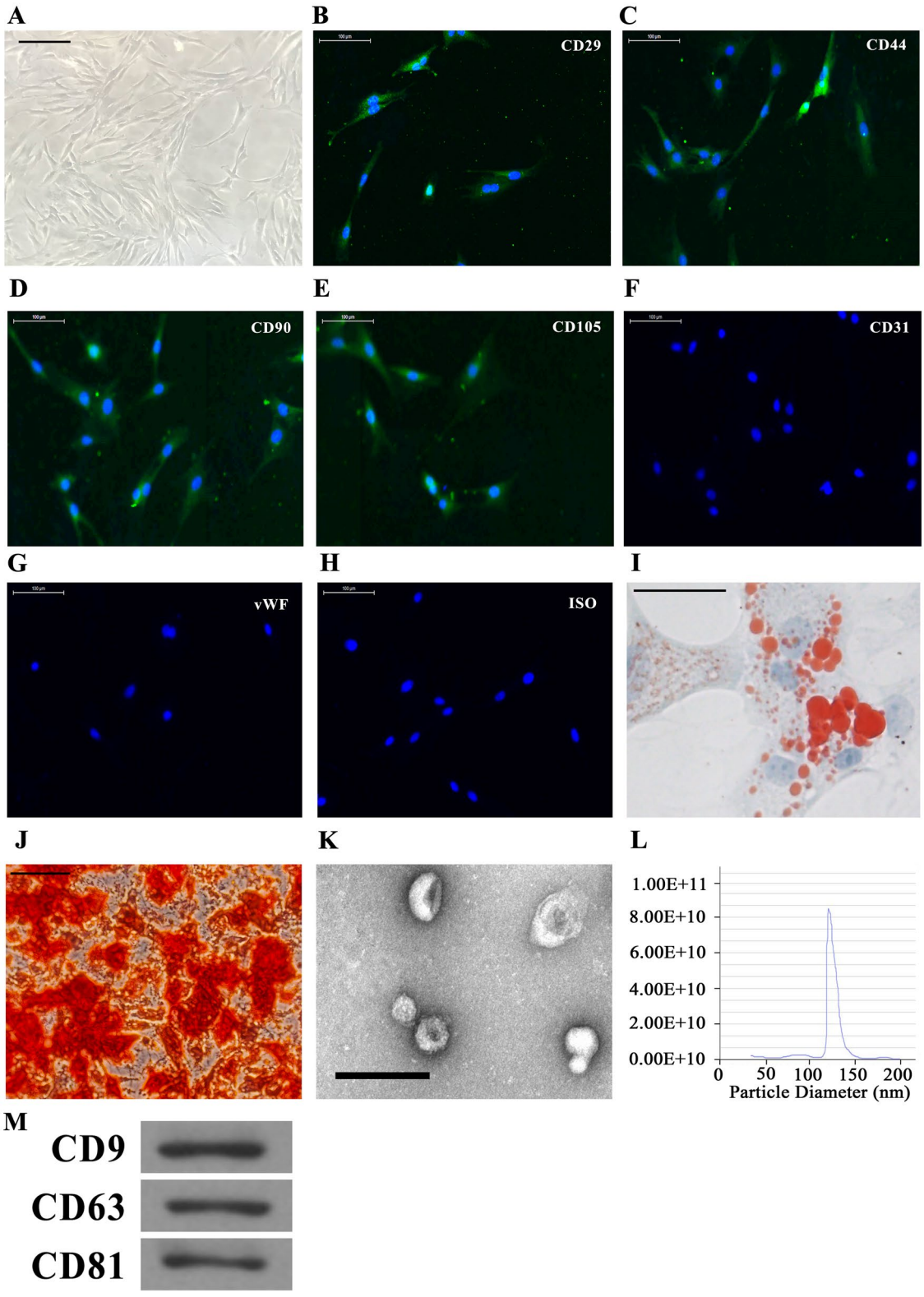
A
B
CD29
C
CD44
D
CD90
E
CD105
F
CD31
G
vWF
H
ISO
I
J
K
L
1.00E+11
8.00E+10
6.00E+10
4.00E+10
2.00E+10
0.00E+10
0
50
100
150
200
Particle Diameter (nm)
M
CD9
CD63
CD81

◂**Fig. 1** Characterization of exosomes released by adipose-derived stem cells (ADSCs). **A** ADSCs showed a typical cobblestone-like morphology. Scale bar: 100 μm. **B–H** Immunofluorescence staining of cell surface markers. Antibodies were labeled with fluorescein isothiocyanate (FITC, green). Cell nuclei were stained with DAPI (blue). CD29, CD90, CD44, and CD105 are positive. CD34 and von Willebrand Factor (vWF) are negative. FITC-labeled mouse IgG isotype controls are shown (×400). Scale bar: 100 μm. **I**, **J** Differentiation potential of ADSCs assessed by Oil-Red O (**I**) and alkaline phosphatase staining (**J**). Scale bar: 100 μm. **K** Transmission electron micrographs showing ADSC exosome morphology. Scale bar: 200 nm. **L** Particle size distribution and concentration of ADSC exosomes measured by tunable resistive pulse sensing. **M** Western blotting of CD9, CD63, and CD81 expression in ADSC-derived exosomes.

GUUG-3′, *miR-490-3p* reverse, 5′-CAGUACUUUUGUGUAGUACAA-3′, *SIRT3* forward, 5′-CTGGATGGACAGGACAGATAAG-3′, *SIRT3* reverse, 5′-TCTTGCTGGACATAGGATGATC-3′, *U6* forward, 5′-GCTTCGGCAGCACATATACTAAAAT-3′, *U6* reverse, 5′-CGCTTCACGAATTTGCGTGTCAT-3′, *GAPDH* forward, 5′-TGCTGAGTATGTCGTGGAGTCT-3′, and *GAPDH* reverse, 5′-ATGCATTGCTGACAATCTTGAG-3′.

### Luciferase Reporter Assay

We cloned wild-type (WT) and 3′-UTR mutant (MUT) *SIRT3* and *circ-Fryl* into the pMIR firefly luciferase-expressing vector. We cotransfected HEK293T cells at 70% confluence with 500 ng pMIR-SIRT3-wt/pMIR-SIRT3-Mut or pMIR-*circ-Fryl*-wt/pMIR-*circ-Fryl*-Mut along with miR-490-3p mimics of 50 nM via the Lipofectamine 2000 Transfection Kit (Thermo Fisher Scientific). We assayed luciferase activity through the Dual-Luciferase Reporter System (Promega, Madison, WI, USA). We performed 5 independent assays.

### Western Blotting

Proteins were extracted using radioimmunoprecipitation assay lysis buffer (sc-24948). Proteins (20 μg) were separated by SDS-PAGE, which were transferred to PVDF membrane and was probed with primary antibodies against CD9, CD63, CD81, caspase-3, LC-3, SIRT3, and MAPK. We incubated membranes though appropriate secondary antibodies. Immunoreactivity was visualized with the ECL Western Blotting Detection System (Millipore). We performed gray value analyses via UN-Scan-It 6.1 (Silk Scientific Inc., Orem, UT, USA).

### Enzyme-Linked Immunosorbent Assay (ELISA)

We collected cell culture medium following different treatments. We employed ELISA kits (R&D Systems, Minneapolis, MN, USA) to detect interleukin (IL)-6, IL-1β, monocyte chemoattractant protein (MCP)-1, and tumor necrosis factor (TNF)-α levels following standard procedure.

### Statistical Analysis

We denoted continuous variables by means ± standard deviation (SD). We employed one-way variance analysis using GraphPad Prism (GraphPad, La Jolla, CA, USA) to compare differences. $P \leq 0.05$ inferred statistical significance.

## RESULTS

### Exosome and ADSC Characterization

Isolated ADSCs had typical cobblestone-like morphology (Fig. 1A). Immunofluorescence staining verified that mouse adipose tissue ADSCs were positive for the mesenchymal cell surface markers CD29 (Fig. 1B), CD44 (Fig. 1C), CD90 (Fig. 1D), and CD105 (Fig. 1E), while negative for endothelial marker CD34 (Fig. 1F) and von Willebrand Factor (vWF) (Fig. 1G). Oil-Red O (Fig. 1I) and alizarin red (Fig. 1J) staining revealed that isolated ADSCs had adipocyte and osteoblast differentiation ability. We verified that ADSCs had multidirectional differentiation functions like formerly investigated [14, 15].

We isolated exosomes through ultra-high speed centrifugation. Transmission electron micrographs demonstrated that ADSC-derived exosomes had a cup-shaped or spherical morphology (Fig. 1K), approximately 100 nm in diameter (Fig. 1L), consistent with previous studies [16, 17]. Western blotting suggested that ADSC exosomes were positive regarding exosome marker protein expression including CD63, CD9, and CD81, which are cellular components as well (Fig. 1M).

### Circ-Fryl Plays a Role in ADSC Exosome-Mediated Attenuation of Sepsis-Induced Lung Injury

Several studies have found that ADSC exosomes (ADSC-EVs) have therapeutic effects for many diseases

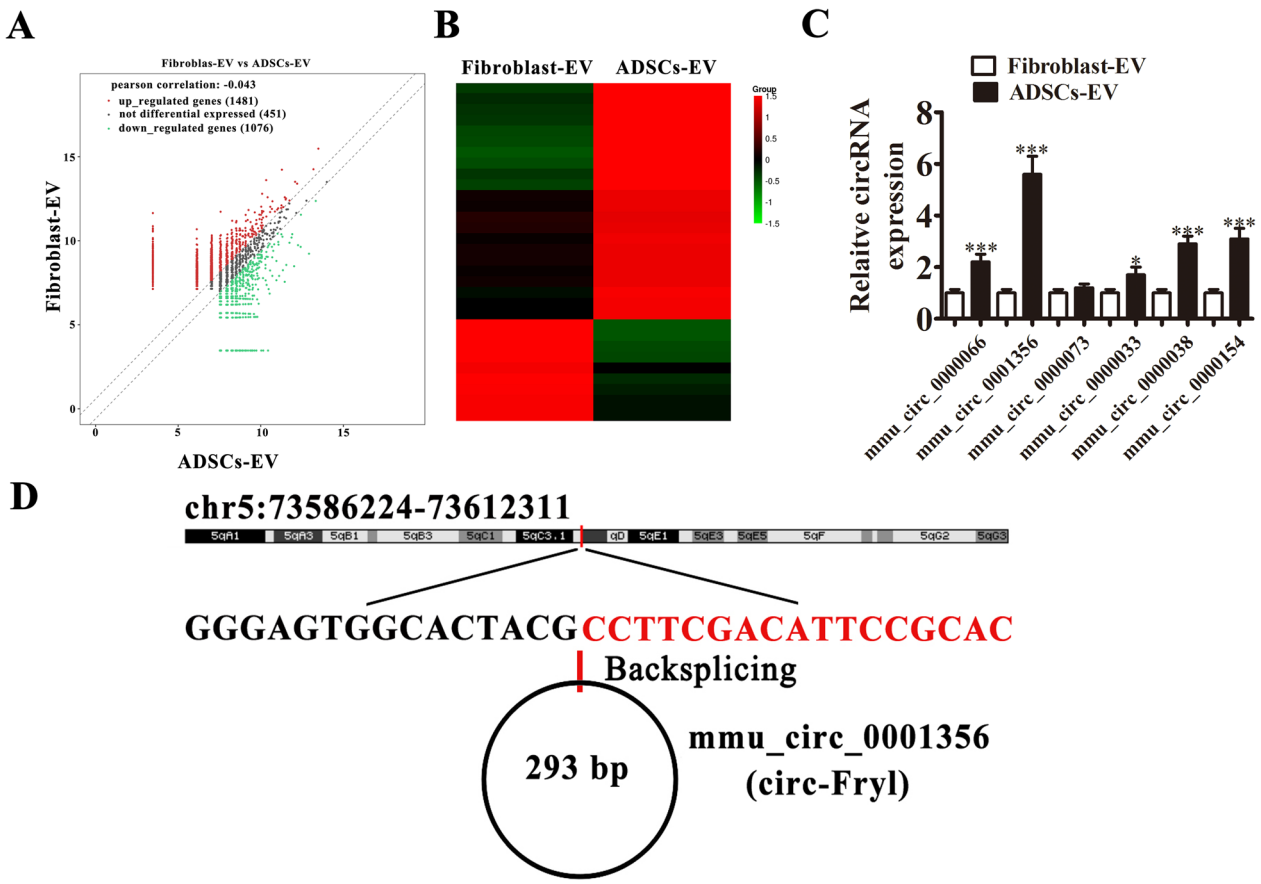
A
Fibroblas-EV vs ADSCs-EV
pearson correlation: -0.043
up_regulated genes (1481)
not differential expressed (451)
down_regulated genes (1076)
Fibroblast-EV
ADSCs-EV
B
Fibroblast-EV
ADSCs-EV
Group
C
Fibroblast-EV
ADSCs-EV
Relaitve circRNA expression
mmu_circ_0000066
mmu_circ_0001356
mmu_circ_0000073
mmu_circ_0000033
mmu_circ_0000038
mmu_circ_0000154
D
chr5:73586224-73612311
GGGAGTGGCACTACGCCTTCGACATTCCGCAC
Backsplicing
293 bp
mmu_circ_0001356
(circ-Fryl)
E
Relaitve circ-Fryl expression
NC
si-circ-Fryl
F
Ctrl
sepsis
sepsis+ADSCs-EV
sepsis+sicirc-ADSCs-EV
G
Relaitve apoptosis ratio
NC
sepsis
sepsis+ADSCs-EV
sepsis+sicirc-ADSCs-EV

◂**Fig. 2** Circ-Fryl plays a role in ADSC exosome (ADSC-EV) attenuation of sepsis-induced lung injury. **A** Total differential expression of circular RNAs (circRNAs). **B** Heat map of circRNAs in fibroblast and ADSC exosomes. **C** RT-qPCR shows the expression of the six most significantly upregulated circRNAs. Data are presented as mean ± standard deviation (SD); $^{*}P < 0.05$, $^{***}P < 0.001$ vs. the fibroblast-derived exosome group. **D** Genomic loci of the *Fryl* gene and circ-Fryl (mmu_circ_0001356). **E** RT-qPCR shows the expression of circ-Fryl in ADSC-EVs after transfection with negative control (NC) or small interfering RNA (siRNA) against circ-Fryl. Data are presented as mean ± SD; $^{***}P < 0.001$ vs. NC group. **F**, **G** Immunohistochemical and TUNEL staining show that downregulation of circ-Fry1 attenuates the protective effect of ADSC-EVs in sepsis-induced lung injury. Data are presented as mean ± SD; $^{***}P < 0.001$ vs. ctrl group, $^{\#\#\#}P < 0.001$ vs. ADSC-EV group. Ctrl, control.

[17, 18]. Nevertheless, the ADSC-EV role in sepsis-induced lung injury is unclear. CircRNAs make up a large group of non-coding RNAs and function in a variety of disease pathologies, including sepsis-induced acute lung injury [19]. To determine the therapeutic mechanism, the total differential expression of circRNAs in exosomes derived from fibroblasts or ADSCs was identified by high-throughput sequencing. A total of 1481 circRNAs were upregulated and 1076 circRNAs were downregulated in ADSC-EVs compared with fibroblast exosomes (Fig. 2A and B). RT-qPCR was employed to confirm the six most significantly upregulated circRNAs; circ-Fryl (mmu_circ_0001356) had the highest expression (Fig. 2C). We determined that circ-Fryl was derived and cyclized from a portion of the *Fryl* gene exon and was located at chr5:73,586,224–73,612,311 (Fig. 2D).

To identify the role of circ-Fryl, ADSCs were transfected with negative control (NC) or siRNA circ-Fryl (si-circ-Fryl) vector. RT-qPCR showed that circ-Fryl in si-circ-Fryl ADSC-EVs decreased significantly compared with the NC group (Fig. 2E). Immunohistochemical and TUNEL staining showed that ADSC-EV treatment decreased sepsis-induced AEC apoptosis. Downregulation of circ-Fry1 attenuated the protective effect of ADSC-EVs in sepsis-induced lung injury (Fig. 2F and G), suggesting that circ-Fry1 plays an important role in ADSC exosome-mediated attenuation of sepsis-induced lung injury.

## Exosomes from Circ-Fryl-Silenced ADSCs Exhibited a Decreased Therapeutic Effect in Sepsis-Induced Lung Injury by Recovery of Inflammatory Factor Expression

ELISA detection showed the inflammatory factors IL-1β, TNF-α, IL-6, and MCP-1 in alveolar lavage fluid were significantly increased in the sepsis-induced mouse model; treatment with ADSC-EVs decreased levels of IL-1β, TNF-α, IL-6, and MCP-1. Exosomes derived from circ-Fryl-silenced ADSCs exhibited a decreased therapeutic effect in sepsis-induced lung injury by recovery of inflammatory factor expression (Fig. 3A–D). Western blotting showed that ADSC-EV treatment decreased sepsis-induced caspase-3 expression, while circ-Fryl silencing decreased the inhibitory effect of ADSC-EVs on caspase-3 expression (Fig. 3E). Further analysis showed that ADSC-EV treatment promoted autophagy activation by promoting LC3-II/LC3-I expression in lung tissues while silencing of circ-Fryl decreased autophagy activation (Fig. 3F). ADSC-EV treatment also promoted SIRT3 and AMPK expression, but circ-Fryl silencing decreased SIRT3/AMPK signal (Fig. 3G and H).

## SIRT3 and miR-490-3p Are Downstream Targets of Circ-Fryl

Bioinformatics analysis suggested that miR-490-3p was circ-Fryl downstream target. Luciferase reporter assays suggested that miR-490-3p is also circ-Fryl downstream target (Fig. 4A) and circ-Fryl inhibited luciferase activity in WT yet not MUT cell lines (Fig. 4B). Bioinformatics analysis also indicated that SIRT3 is a miR-490-3p target; miR-490-3p interacted directly with the SIRT3 3′-UTR to suppress expression of its mRNA (Fig. 4C). In luciferase reporter assays, miR-490-3p inhibited luciferase activity in WT while not MUT cell lines (Fig. 4D). These results indicate that circ-Fryl protects against sepsis-induced lung injury by targeting the miR-490-3p/SIRT3 axis.

To characterize interactions among circ-Fryl, miR-490-3p, and SIRT3, AECs were transfected with negative control (NC), siRNA against circ-Fryl (si-circ-Fryl), miR-490-3p inhibitor, and SIRT3 overexpression vector alone or in combination. RT-qPCR showed that downregulation of circ-Fryl suppressed circ-Fryl expression; downregulation of circ-Fryl or overexpression of SIRT3 could not recover circ-Fryl expression following circ-Fryl silencing in AECs (Fig. 4E). Downregulation of circ-Fryl also promoted miR-490-3p expression. Following miR-490-3p inhibitor treatment, miR-490-3p expression was suppressed in AECs. Upregulation of SIRT3 did not suppress miR-490-3p expression following silencing of circ-Fryl (Fig. 4F). RT-qPCR of SIRT3 showed that circ-Fryl

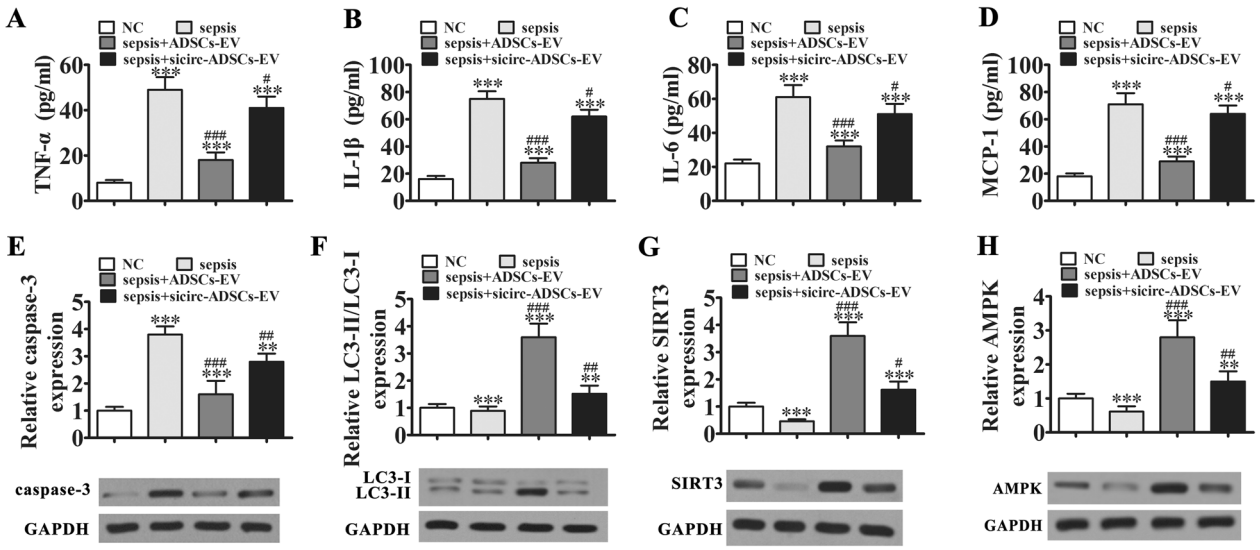


**Fig. 3** Exosomes derived from circ-Fryl silenced ADSCs exhibited decreased therapeutic effects in sepsis-induced lung injury by recovery of inflammatory factor expression. **A**–**D** ELISA shows the expression of TNF-α, IL-1β, IL-6, and MCP-1 in alveolar lavage fluid. Data are presented as mean ± SD; $^{***}P < 0.001$ vs. ctrl group, $^{\#}P < 0.05$, $^{\#\#\#}P < 0.001$ vs. ADSC-EV group. **D** Western blotting shows expression of the apoptosis-related protein caspase-3. Data are presented as mean ± SD; $^{**}P < 0.01$, $^{***}P < 0.001$ vs. ctrl group, $^{\#\#}P < 0.01$, $^{\#\#\#}P < 0.001$ vs. ADSC-EV group. **F**–**H** Western blotting shows expression of the autophagy and signaling pathway-related proteins LC3 (**F**), SIRT3 (**G**), and MAPK (**H**). Data are presented as mean ± SD; $^{**}P < 0.01$, $^{***}P < 0.001$ vs. ctrl group, $^{\#}P < 0.05$, $^{\#\#}P < 0.01$, $^{\#\#\#}P < 0.001$ vs. ADSC-EV group.

silencing suppressed SIRT3 expression. Downregulation of miR-490-3p recovered SIRT3 expression, and SIRT3 overexpression promoted SIRT3 expression in AECs (Fig. 4G). Altogether, our results show that circ-Fryl can promote SIRT3 expression by adsorption of miR-490-3p.

## miR-490-3p or Silencing SIRT3 Expression Suppressed Protective Effect of Circ-Fryl in LPS Conditions

To determine if circ-Fryl regulated the survival of AECs by regulating miR-490-3p/SIRT3, AECs were transfected with circ-Fryl overexpression vector, miR-490-3p mimic, or SIRT3 silencing alone or in combination prior to exposure to LPS. AEC apoptosis was detected by immunofluorescence. miR-490-3p overexpression or SIRT3 silencing suppressed circ-Fryl protective effects in LPS-induced apoptosis (Fig. 5A and B). Autophagy plaques of AECs detected by immunofluorescence showed that miR-490-3p overexpression or SIRT3 silencing suppressed the autophagosome formation even with upregulation of circ-Fryl (Fig. 5C and D). ELISA detection showed that miR-490-3p overexpression or SIRT3 silencing reversed circ-Fryl inhibitory effect on inflammatory factors IL-1β, IL-6, TNF-α, and MCP-1 (Fig. 5E–H). Western blotting validated that circ-Fryl overexpression suppressed caspase-3 expression, while miR-490-3p overexpression or SIRT3 silencing recovered caspase-3 levels (Fig. 5I). Western blotting also showed that circ-Fryl overexpression increased LC3-II/LC3-I, SIRT3, and AMPK levels, while miR-490-3p overexpression or SIRT3 silencing suppressed LC3-II/LC3-I, SIRT3, and AMPK expression even in the presence of circ-Fryl overexpression (Fig. 5J–L), suggesting that miR-490-3p overexpression or SIRT3 silencing suppressed circ-Fryl protective effect following treatment with LPS by regulating autophagy.

## DISCUSSION

Sepsis is a popular critical and acute disease, which is characterized by sustained hypotension, metabolic acidosis, and SIRS [20]. It can cause multiple organ injuries and mortality. Because of the pulmonary susceptibility, acute lung injury is a usual lethal sepsis complication

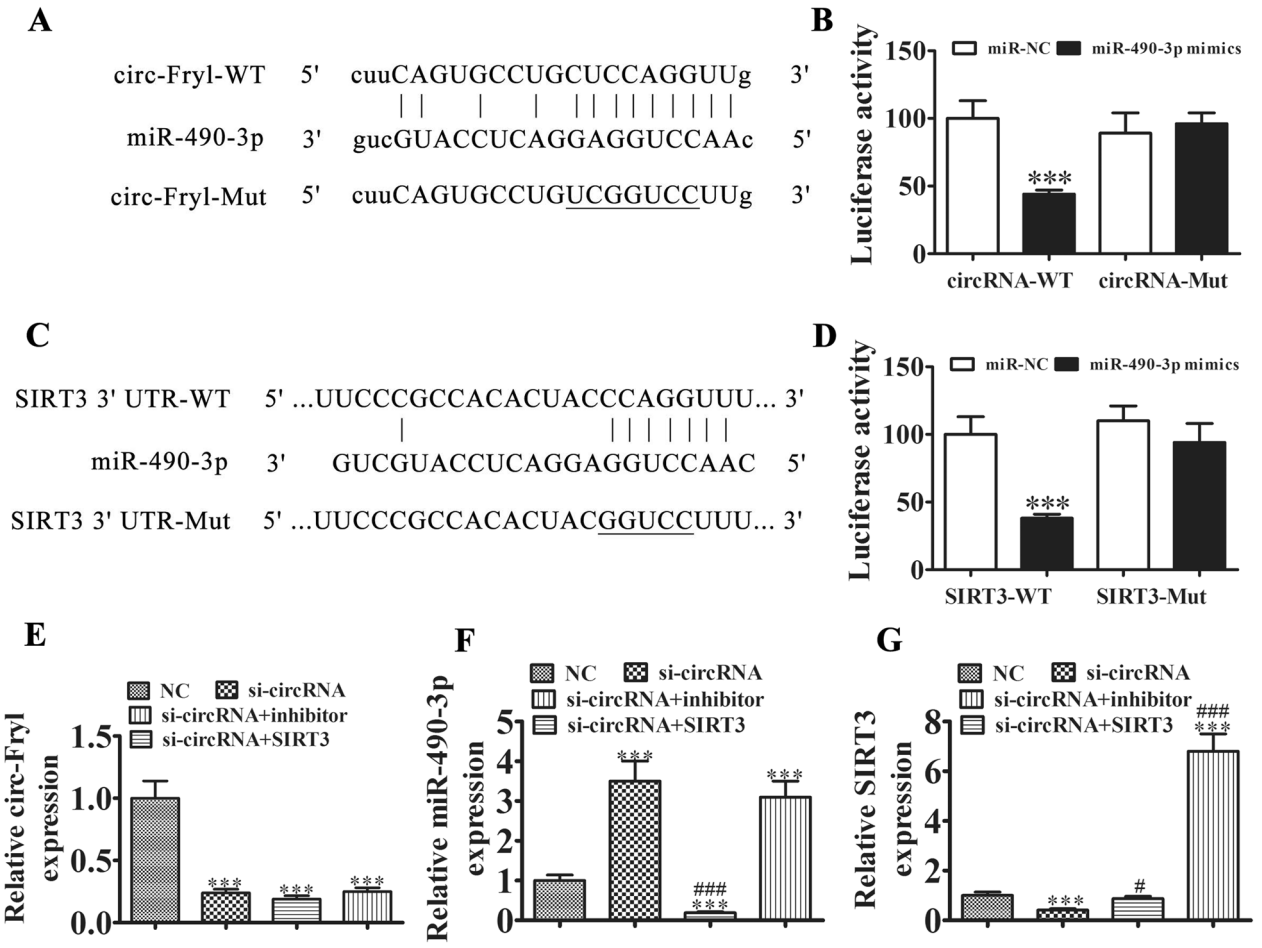


**Fig. 4** miR-490-3p and SIRT3 are downstream targets of circ-Fryl. **A** Prediction of the binding sites of miR-490-3p in circ-Fryl. The mutant (MUT) version of circ-Fryl is presented. **B** Relative luciferase activity determined 48 h following transfection of HEK293T cells with miR-490-3p mimic/NC or circ-Fryl WT/Mut. Data are presented as means ± SD. $^{***}P < 0.001$. **C** Prediction of binding sites of miR-490-3p within the 3′UTR of SIRT3. The MUT version of 3′-UTR-SIRT3 is shown. **D** Relative luciferase activity determined 48 h following transfection of HEK293T cells with miR-490-3p mimic/NC or 3′UTR-SIRT3 WT/MUT. Data are presented as means ± SD. $^{***}P < 0.001$. **E**–**G** RT-qPCR shows the expression of circ-Fryl, miR-490-3p, and SIRT3. Data are presented as mean ± SD; $^{***}P < 0.001$ vs. NC group, $^{\#}P < 0.05$, $^{\#\#\#}P < 0.001$ vs. si-circRNA group.

[21]. Previous investigations have found that exosomes, biological lipid bilayer nanoparticles secreted through the endosomal pathway, which recently emerged as essential cargos that carry multiple mediators, are fundamental in sepsis-associated organ dysfunction pathogenesis [22]. Mesenchymal stem cell exosomes have been shown to alleviate sepsis-associated multiple organ injury [23]. Current investigations have also suggested that ADSC exosomes have protective effects in sepsis-induced lung injury by suppressing inflammatory factor expression, but the underlying mechanism remains unclear.

CircRNA function is important in regulation of the microenvironment after sepsis [19]. To determine the protective mechanism of ADSC exosomes in sepsis-induced lung injury, high-throughput sequencing was used to compare circRNA expression in ADSC exosomes and fibroblast exosomes. ADSC exosomes exhibited increased expression of circ-Fryl compared with fibroblast exosomes. Downregulation of circ-Fryl inhibited ADSC exosome protective effect in sepsis-induced lung injury, suggesting that circ-Fryl plays an essential role in ADSC exosome-mediated therapeutic effects.

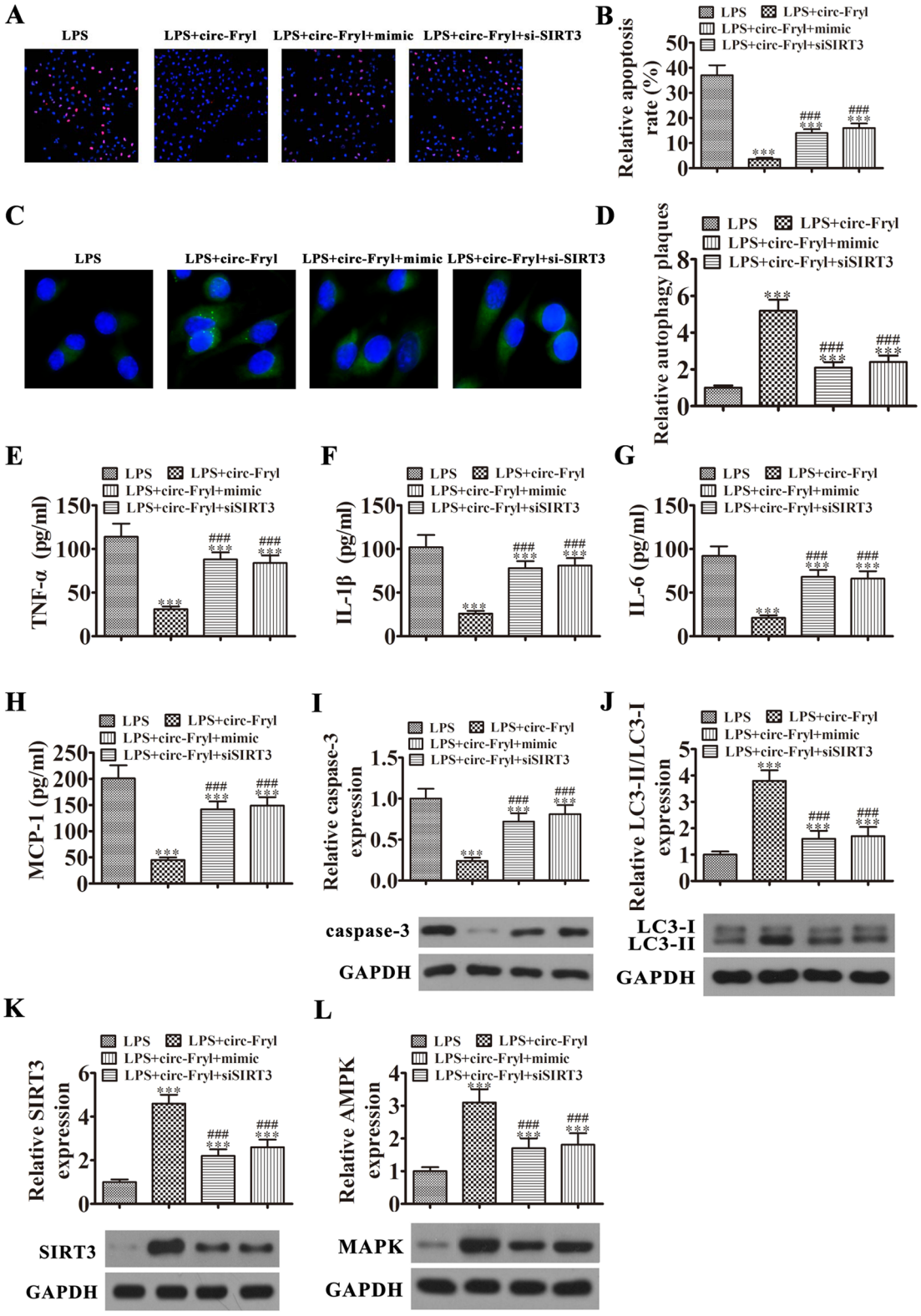
A
LPS
LPS+circ-Fryl
LPS+circ-Fryl+mimic
LPS+circ-Fryl+si-SIRT3
B
Relative apoptosis rate (%)
C
D
Relative autophagy plaques
E
TNF-α (pg/ml)
F
IL-1β (pg/ml)
G
IL-6 (pg/ml)
H
MCP-1 (pg/ml)
I
Relative caspase-3 expression
caspase-3
GAPDH
J
Relative LC3-II/LC3-I expression
LC3-I
LC3-II
GAPDH
K
Relative SIRT3 expression
SIRT3
GAPDH
L
Relative AMPK expression
MAPK
GAPDH

◂**Fig. 5** Overexpression of miR-490-3p or silencing of SIRT3 suppressed the protective effect of circ-Fryl following LPS treatment. **A**, **B** Alveolar epithelial cell (AEC) apoptosis was detected by immunofluorescence. Data are presented as mean ± SD; $^{***}P < 0.001$ vs. LPS group, $^{\#\#\#}P < 0.001$ vs. circ-Fryl group. **C**, **D** Autophagy plaques of AECs were detected. Data are presented as mean ± SD; $^{***}P < 0.001$ vs. LPS group, $^{\#\#\#}P < 0.001$ vs. circ-Fryl group. **E**–**H** ELISA shows expression of TNF-α, IL-1β, IL-6, and MCP-1. Data are presented as mean ± SD; $^{***}P < 0.001$ vs. LPS group, $^{\#\#\#}P < 0.001$ vs. circ-Fryl group. **I**–**L** Western blotting shows the expression of caspase-3 (**I**), LC3 (**J**), SIRT3 (**K**), and MAPK (**L**). Data are presented as mean ± SD; $^{***}P < 0.001$ vs. LPS group, $^{\#\#\#}P < 0.001$ vs. circ-Fryl group.

Bioinformatic analyses revealed miR-490-3p and SIRT3 as downstream targets of circ-Fryl. Luciferase reporter assays confirmed the correlation between miR-490-3p, SIRT3, and circ-Fryl, indicating that ADSC exosomes can deliver circ-Fryl to AECs, which promotes SIRT3 expression by adsorption of miR-490-3p. RT-qPCR confirmed that downregulation of circ-Fryl promoted miR-490-3p and inhibited SIRT3 expression. Our in vitro experiments also showed that overexpression of circ-Fryl suppressed LPS-induced AEC apoptosis and inflammatory factor expression. Overexpression of miR-490-3p or downregulation of SIRT3 recovered AEC apoptosis and inflammatory factor expression following LPS induction.

We also found that autophagy plays a role in protection against ADSC exosome-mediated lung injury. Previous studies have found that activation of autophagy has a protective effect in sepsis-induced organ injury induced by suppressed stress pathway inactivation [24]. The SIRT3/AMPK/autophagy network orchestrates the protective effects of stressed induced organ injuries [25]. SIRT3 overexpression promoted autophagy by upregulation of AMPK [26]. Our study also found that overexpression of circ-Fryl promoted autophagy by upregulating SIRT3/AMPK signaling, indicating that exosomes derived from ADSCs attenuate sepsis-induced lung injury via delivery of circ-Fryl and regulation of the miR-490-3p/SIRT3 pathway mediated autophagy activation.

## CONCLUSIONS

This study demonstrated the potential of exosomes as a new therapeutic option regarding sepsis-induced lung injury. Exosomes derived from ADSCs attenuated sepsis-induced lung injury by circ-Fryl delivery and regulation of the miR-490-3p/SIRT3 pathway mediated activation of autophagy. But if there are other ways that circ-Fryl regulation autophagy beside SIRT3 still unclear and need clarify in the following study.

## AUTHOR CONTRIBUTION

The study was designed, and funding was provided by WS; the study was conducted, and the manuscript was prepared by XZ; most experiments were performed by WS; the data were studied by SL; and samples were provided by SL. The final manuscript was read and approved by all authors.

## FUNDING

This study was supported by the National Natural Science Foundation of China (Grant no. 81772121).

## AVAILABILITY OF DATA AND MATERIALS

The datasets used and/or analyzed in the current study are available from the corresponding author upon reasonable request.

## DECLARATIONS

**Ethics Approval and Consent to Participate** The Animal Care and Use Committee of the Shanghai Tenth People's Hospital approved the research. We conducted postoperative animal care and treatment surgical interventions according to NIH Guide of Laboratory Animals Care and Use.

**Consent for Publication** All authors agree to publish this article.

**Competing Interests** The authors declare no competing interests.

## REFERENCES

1. Christ-Crain, M., N.G. Morgenthaler, J. Struck, S. Harbarth, A. Bergmann, and B. Muller. 2005. Mid-regional pro-adrenomedullin as a prognostic marker in sepsis: An observational study. *Critical Care* 9: R816–R824.
2. Lou, L., D. Hu, S. Chen, S. Wang, Y. Xu, Y. Huang, et al. 2019. Protective role of JNK inhibitor SP600125 in sepsis-induced acute lung injury. *International Journal of Clinical and Experimental Pathology* 12: 528–538.
3. Jang, E.A., J.Y. Kim, T.D. Tin, J.A. Song, S.H. Lee, and S.H. Kwak. 2019. The effects of BMS-470539 on lipopolysaccharide-induced acute lung injury. *Acute Crit Care* 34: 133–140.

4. Janicova, A., N. Becker, B. Xu, S. Wutzler, J.T. Vollrath, F. Hildebrand, et al. 2019. Endogenous uteroglobin as intrinsic anti-inflammatory signal modulates monocyte and macrophage subsets distribution upon sepsis induced lung injury. *Frontiers in Immunology* 10: 2276.
5. Yen, Y.T., H.R. Yang, H.C. Lo, Y.C. Hsieh, S.C. Tsai, C.W. Hong, et al. 2013. Enhancing autophagy with activated protein C and rapamycin protects against sepsis-induced acute lung injury. *Surgery* 153: 689–698.
6. Wang, W., X. Yang, Q. Chen, M. Guo, S. Liu, J. Liu, et al. 2020. Sinomenine attenuates septic-associated lung injury through the Nrf2-Keap1 and autophagy. *Journal of Pharmacy and Pharmacology* 72: 259–270.
7. Chen, H.H., P.F. Lai, Y.F. Lan, C.F. Cheng, W.B. Zhong, Y.F. Lin, et al. 2014. Exosomal ATF3 RNA attenuates pro-inflammatory gene MCP-1 transcription in renal ischemia-reperfusion. *Journal of Cellular Physiology* 229: 1202–1211.
8. Chen, K.H., C.H. Chen, C.G. Wallace, C.M. Yuen, G.S. Kao, Y.L. Chen, et al. 2016. Intravenous administration of xenogenic adipose-derived mesenchymal stem cells (ADMSC) and ADMSC-derived exosomes markedly reduced brain infarct volume and preserved neurological function in rat after acute ischemic stroke. *Oncotarget* 7: 74537–74556.
9. Fleig, S.V., and B.D. Humphreys. 2014. Rationale of mesenchymal stem cell therapy in kidney injury. *Nephron Clinical Practice* 127: 75–80.
10. Geng, W., H. Tang, S. Luo, Y. Lv, D. Liang, X. Kang, et al. 2019. Exosomes from miRNA-126-modified ADSCs promotes functional recovery after stroke in rats by improving neurogenesis and suppressing microglia activation. *American Journal of Translational Research* 11: 780–792.
11. Shang, Y., Y. Sun, J. Xu, X. Ge, Z. Hu, J. Xiao, et al. 2020. Exosomes from mmu_circ_0001359-modified ADSCs attenuate airway remodeling by enhancing FoxO1 signaling-mediated M2-like macrophage activation. *Molecular Therapy-Nucleic Acids* 19: 951–960.
12. Meng, L., H. Cao, C. Wan, and L. Jiang. 2019. MiR-539-5p alleviates sepsis-induced acute lung injury by targeting ROCK1. *Folia Histochemica et Cytobiologica* 57: 168–178.
13. Zhang, Y.Y., X. Liu, X. Zhang, and J. Zhang. 2020. Shikonin improve sepsis-induced lung injury via regulation of miRNA-140-5p/TLR4—A vitro and vivo study. *Journal of Cellular Biochemistry* 121: 2103–2117.
14. Jin, J., Y. Wang, L. Zhao, W. Zou, M. Tan, and Q. He. 2020. Exosomal miRNA-215-5p derived from adipose-derived stem cells attenuates epithelial-mesenchymal transition of podocytes by inhibiting ZEB2. *BioMed Research International* 2020: 2685305.
15. Avila-Portillo, L.M., F. Aristizabal, A. Riveros, M.C. Abba, and D. Correa. 2020. Modulation of adipose-derived mesenchymal stem/stromal cell transcriptome by G-CSF stimulation. *Stem Cells International* 2020: 5045124.
16. Chen, J., and M. Chopp. 2018. Exosome therapy for stroke. *Stroke* 49: 1083–1090.
17. Yang, F., X. Liao, Y. Tian, and G. Li. 2017. Exosome separation using microfluidic systems: size-based, immunoaffinity-based and dynamic methodologies. *Biotechnologu Journal* 12.
18. He, C., S. Zheng, Y. Luo, and B. Wang. 2018. Exosome theranostics: Biology and translational medicine. *Theranostics* 8: 237–255.
19. Bao, X., Q. Zhang, N. Liu, S. Zhuang, Z. Li, Q. Meng, et al. 2019. Characteristics of circular RNA expression of pulmonary macrophages in mice with sepsis-induced acute lung injury. *Journal of Cellular and Molecular Medicine* 23: 7111–7115.
20. Cinar, I., B. Sirin, P. Aydin, E. Toktay, E. Cadirci, I. Halici, et al. 2019. Ameliorative effect of gossypin against acute lung injury in experimental sepsis model of rats. *Life Sciences* 221: 327–334.
21. Cadirci, E., B.Z. Altunkaynak, Z. Halici, F. Odabasoglu, M.H. Uyanik, C. Gundogdu, et al. 2010. Alpha-lipoic acid as a potential target for the treatment of lung injury caused by cecal ligation and puncture-induced sepsis model in rats. *Shock* 33: 479–484.
22. Park, E.J., M.G. Appiah, P.K. Myint, A. Gaowa, E. Kawamoto, and M. Shimaoka. 2019. Exosomes in sepsis and inflammatory tissue injury. *Current Pharmaceutical Design* 25: 4486–4495.
23. Zhang, R., Y. Zhu, Y. Li, W. Liu, L. Yin, S. Yin, et al. 2020. Human umbilical cord mesenchymal stem cell exosomes alleviate sepsis-associated acute kidney injury via regulating microRNA-146b expression. *Biotechnology Letters* 42: 669–679.
24. Chen, H.G., H.Z. Han, Y. Li, Y.H. Yu, and K.L. Xie. 2020. Hydrogen alleviated organ injury and dysfunction in sepsis: The role of cross-talk between autophagy and endoplasmic reticulum stress: Experimental research. *International Immunopharmacol* 78: 106049.
25. Duan, W.J., Y.F. Li, F.L. Liu, J. Deng, Y.P. Wu, W.L. Yuan, et al. 2016. A SIRT3/AMPK/autophagy network orchestrates the protective effects of trans-resveratrol in stressed peritoneal macrophages and RAW 2647 macrophages. *Free Radical Biology and Medicine* 95: 230–242.
26. Zhao, W., L. Zhang, R. Chen, H. Lu, M. Sui, Y. Zhu, et al. 2018. SIRT3 protects against acute kidney injury via AMPK/mTOR-regulated autophagy. *Frontiers in Physiology* 9: 1526.